

Polarization behaviors of (Bi 3.15 Nd 0.85) Ti 3 O 12 thin films deposited by radio-frequency magnetron sputtering

X. S. Gao, J. M. Xue, and J. Wang

Citation: [Journal of Applied Physics](#) **98**, 104106 (2005); doi: 10.1063/1.2131192

View online: <http://dx.doi.org/10.1063/1.2131192>

View Table of Contents: <http://scitation.aip.org/content/aip/journal/jap/98/10?ver=pdfcov>

Published by the [AIP Publishing](#)

Articles you may be interested in

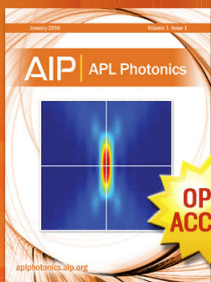
[Fatigue behavior of heterostructured Pb \(Zr , Ti \) O 3 / \(Bi , Nd \) 4 Ti 3 O 12 ferroelectric thin films](#)
Appl. Phys. Lett. **89**, 122905 (2006); 10.1063/1.2347697

[Ferroelectric behaviors and charge carriers in Nd-doped Bi 4 Ti 3 O 12 thin films](#)
J. Appl. Phys. **97**, 034101 (2005); 10.1063/1.1834986

[Structural and dielectric characterization of the \(Ba 1-x Sr x \) \(Ti 0.9 Sn 0.1 \) O 3 thin films deposited on Pt / Ti / SiO 2 / Si substrate by radio frequency magnetron sputtering](#)
J. Appl. Phys. **92**, 2100 (2002); 10.1063/1.1492002

[Growth and characterization of radio-frequency magnetron sputtered lead zirconate titanate thin films deposited on <111> Pt electrodes*](#)
J. Vac. Sci. Technol. A **16**, 2876 (1998); 10.1116/1.581434

[Effect of bismuth on the ferroelectric properties of SrBi 2 Ta 2 O 9 thin films deposited on Pt/SiO 2 /Si by a modified radio-frequency magnetron sputtering technique](#)
J. Vac. Sci. Technol. A **16**, 2505 (1998); 10.1116/1.581373



Launching in 2016!
The future of applied photonics research is here

AIP | APL
Photonics

Polarization behaviors of $(\text{Bi}_{3.15}\text{Nd}_{0.85})\text{Ti}_3\text{O}_{12}$ thin films deposited by radio-frequency magnetron sputtering

X. S. Gao, J. M. Xue, and J. Wang^{a)}*Department of Materials Science and Engineering, Faculty of Engineering, National University of Singapore, Singapore 117576*

(Received 17 May 2005; accepted 9 October 2005; published online 23 November 2005)

Ferroelectric $(\text{Bi}_{3.15}\text{Nd}_{0.85})\text{Ti}_3\text{O}_{12}$ (BNdT) thin films of random orientation have been successfully deposited on Pt/Ti/SiO₂/Si(001) by radio-frequency magnetron sputtering, followed by rapid thermal annealing at 700 °C. They exhibit a remanent polarization $2P_r$ of 23.2 $\mu\text{C}/\text{cm}^2$ and a coercive field E_C of 112 kV/cm at an applied voltage of 10 V. These BNdT films also show a switchable polarization ($\Delta P = P_{\text{sw}} - P_{\text{ns}}$) of 12.9 $\mu\text{C}/\text{cm}^2$ at 5 V, together with an almost fatigue-free behavior up to 1.4×10^{10} switching cycles at both 100 and 150 °C. They demonstrate desirable retention and imprint behaviors at 100 °C, while a further increase in temperature up to 150 °C led to an acceleration in both retention loss and imprint behavior, which can be accounted for by the thermally assisted redistribution of defects and space charges. Studies of the ac dependence of relative permittivity suggest the occurrence of domain-wall pinning, which is a commonly observed phenomenon in oxide ferroelectric thin films. © 2005 American Institute of Physics.

[DOI: [10.1063/1.2131192](https://doi.org/10.1063/1.2131192)]

I. INTRODUCTION

Oxide ferroelectric thin films have been extensively investigated for applications in microelectromechanical systems (MEMSs) and ferroelectric random access memories (FRAMs).^{1–5} In comparison to $\text{Pb}(\text{Zr},\text{Ti})\text{O}_3$ (PZT) and $\text{SrBi}_2\text{Ta}_2\text{O}_9$ (SBT), certain rare-earth-doped $\text{Bi}_4\text{Ti}_3\text{O}_{12}$ of layered perovskite structures demonstrate a much improved fatigue resistance, high retention of nonvolatile polarization, together with a relatively lower processing temperature.^{6–8} Recently, there has been a surge of interest in the investigation of $(\text{Bi},\text{Nd})\text{Ti}_3\text{O}_{12}$ (BNdT), owing to its lead-free composition and excellent polarization behaviors. On the one hand, accordingly, several thin-film deposition techniques have been utilized to synthesize thin films of BNdT-based composition, including pulsed laser deposition (PLD), chemical solution deposition (CSD), and chemical-vapor deposition (CVD).^{9–15} On the other hand, although rf sputtering is widely employed in various semiconductor and device fabrication processes, little has been reported for the deposition of BNdT films by rf sputtering with well-established ferroelectric properties. On the basis of our previous studies, rf sputtering can give rise to $(\text{Bi}_{3.15}\text{Nd}_{0.85})\text{Ti}_3\text{O}_{12}$ thin films of random orientation with desirable ferroelectric behaviors.^{16,17} However, these BNdT thin films have not been properly studied for their polarization and switching behaviors. It is thus of considerable interest to investigate their ferroelectric and dielectric properties, in connection with the polarization and domain switching in these BNdT thin films.

II. EXPERIMENTAL PROCEDURES

The deposition process of the BNdT thin films by rf sputtering was detailed elsewhere.^{16,17} Briefly, the BNdT thin

films were first deposited by rf magnetron (13.56 Hz) sputtering on Pt/Ti/SiO₂/Si(100) substrates from a 2 in. ceramic target of BNdT (with 5% excess Bi for compensation of likely Bi loss). The deposition ambient is pure Ar gas at a pressure range of 10–15 mtorr, with a rf power of 50–100 W. BNdT thin films of ~ 250 nm in thickness were deposited at room temperature, followed by thermal annealing in a rapid thermal annealing furnace at temperatures in the range of 600–750 °C for 5 min.

Phases developed in the BNdT films were identified by x-ray diffraction (XRD, $\text{Cu } K_\alpha$). Film texture and their microstructures were studied using scanning electron microscopy (SEM, Philips, XL 30) and atomic force microscopy (AFM, Di digital instruments). An optical filmetric thickness measurement meter (Filmetrics Inc., USA) was used to measure the film thickness, which was also confirmed using SEM on the cross section of the thin films. Dielectric properties and ac conductivity were measured by an impedance analyzer (Solatron 1261, UK). A Radiant Precision workstation (Radiant Technologies, USA) was employed to characterize the ferroelectric and polarization switching behaviors of the BNdT films. Prior to the electrical measurements, gold electrodes with areas of $3.1 \times 10^{-4} \text{ cm}^2$ were coated by dc sputtering through a mask.

III. RESULTS AND DISCUSSION

BNdT films were deposited by rf sputtering at room temperature and then thermally annealed by rapid thermal annealing in the range of 600–750 °C. Well-established Aurivillius-phase layer structures were formed in the BNdT film annealed at 700 °C, as shown by the XRD pattern in Fig. 1. It exhibits a tetragonal structure with lattice parameters of $a = 5.40 \text{ \AA}$ and $c = 32.8 \text{ \AA}$, together with a rather random grain orientation. Well-established hysteresis loops (insert in Fig. 1) were observed, where the remanent

^{a)}Electronic mail: msewangj@nus.edu.sg

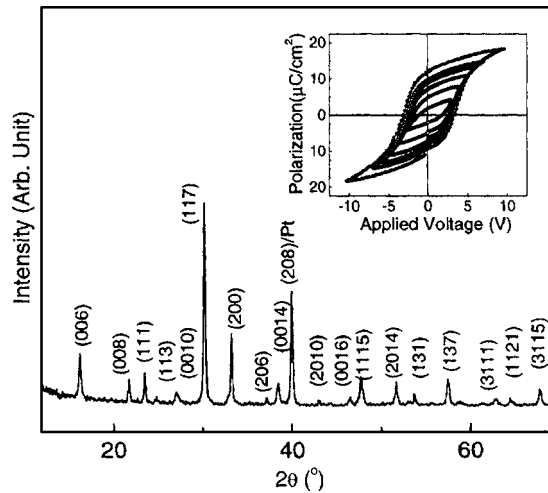


FIG. 1. XRD pattern for the BNdT thin film fabricated by rf magnetron sputtering at room temperature and postannealed at 700 °C. The insert shows the P - E hysteresis loops of this film.

polarization ($2P_r$) and coercive field (E_c) at 10 V were measured to be $23.2 \mu\text{C}/\text{cm}^2$ and 112 kV/cm, respectively.

To further understand the polarization behavior of the BNdT thin films, switchable polarization is plotted against applied pulsed voltage in Fig. 2, where the switchable polarization is defined by $\Delta P = P_{\text{sw}} - P_{\text{ns}}$ (P_{sw} is switching polarization and P_{ns} is nonswitching polarization). As shown in Fig. 2, it increases rather monotonously with rising voltage in the range of 1–12 V, where ΔP values of 12.9 and $19.6 \mu\text{C}/\text{cm}^2$ were obtained at applied voltages of 5 and 10 V, respectively. Although the remanent and switchable polarization values are somehow smaller than those reported for bismuth titanate thin films derived from certain chemical routes, they are comparable to those of the randomly orientated BNdT films deposited by PLD and better than those derived from the sputtering process.^{18–20} Indeed, a degree of preferred grain orientation, which was largely responsible for the high polarization values reported, often took place in the thin films derived from chemical routes and other reported techniques.^{9–15}

As expected, the polarization behaviors of the BNdT thin film deposited by rf sputtering in the present work are de-

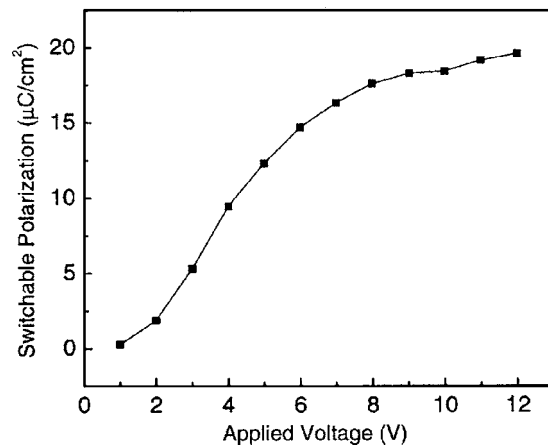


FIG. 2. Switchable polarization ($\Delta P = P_{\text{sw}} - P_{\text{ns}}$) as a function of applied voltage for the BNdT film.

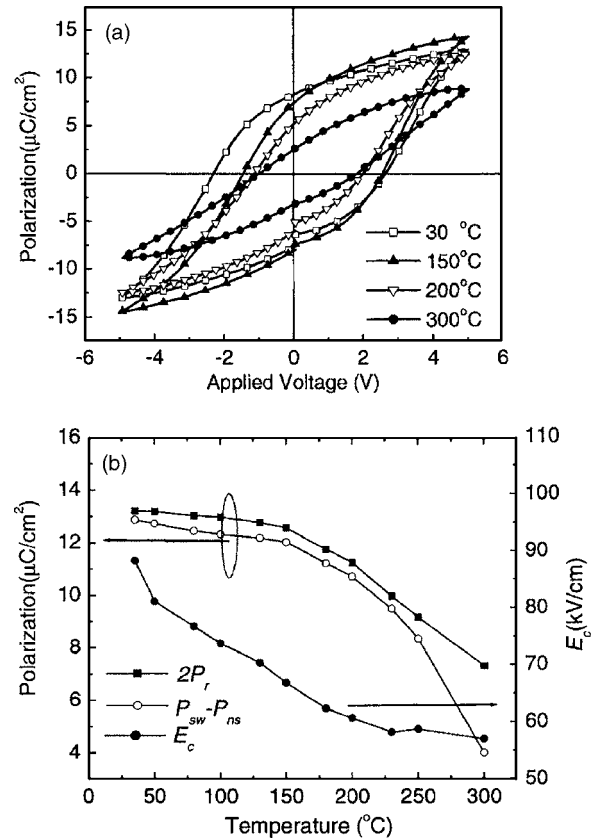


FIG. 3. (a) Hysteresis loops, (b) remanent polarization ($2P_r$), switchable polarization ($\Delta P = P_{\text{sw}} - P_{\text{ns}}$), and coercive field (E_c) as a function of temperature for the BNdT film at 5 V.

pendent on temperature. Figure 3(a) plots the ferroelectric hysteresis loops measured for the BNdT thin film at an operation voltage of 5 V and at temperatures ranging from room temperature to 300 °C. A well-saturated hysteresis loop was shown at room temperature, with a remanent polarization $2P_r$ of $13.2 \mu\text{C}/\text{cm}^2$ and a coercive voltage E_c of 93.2 kV/cm at an operation voltage of 5 V. With increasing temperature, both remanent polarization and coercive field show a decrease. At temperatures above 150 °C, there is an apparent rise in the decreasing rate for both remanent polarization and coercive field. A similar reduction in the switchable polarization (ΔP) at elevated temperatures was observed, as shown in Fig. 3(b), while the BNdT thin film demonstrates desirable temperature-stable polarization and nonvolatile switching behaviors up to 150 °C.

For FRAM applications, BNdT thin films have to be studied for their fatigue behaviors. Figure 4(a) shows the hysteresis loops of the BNdT film derived from rf sputtering before and after the fatigue test using a square bipolar pulse wave at the frequency of 500 kHz at 5 V. It shows a desirable fatigue resistance behavior, and no obvious change was observed after 1.4×10^{10} switching cycles at room temperature. Figure 4(b) plots the evolution of polarizations as a function of switching cycles for the BNdT film. No apparent degradation was observed in the switchable polarization up to 10^{10} switching cycles at room temperature. To accelerate the polarization degradation process, a fatigue test was also performed at 150 °C, which is rather stringent for memory ap-

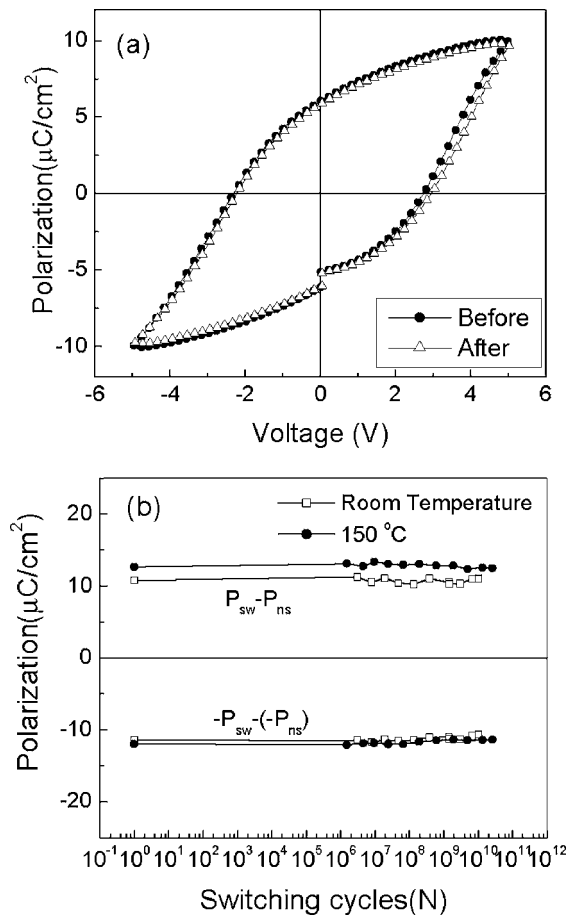


FIG. 4. (a) Hysteresis loops for the BNdT before and after the fatigue test for 1.4×10^{10} polarization switching cycles, and (b) switchable polarizations as a function of polarization switching cycles of fatigue tested at room temperature and 150 °C.

plications. As shown in Fig. 4(b), negligible polarization loss was observed in the long duration test at 150 °C. The fatigue-free behavior of the BNdT derived from rf sputtering is related to the reduced domain-wall pinning effect,²¹ together with the relatively low level of pinning centers in association with defect-induced space charges,^{22–24} which hinder the domain switching. Indeed, $(\text{Bi}_2\text{O}_2)^{2-}$ in the layered perovskites exhibits a net electrical charge, whose positions can be self-regulated as to compensate for other space charges, which has been observed in $\text{SrBi}_2\text{Ta}_2\text{O}_9$.³ This was supported by the impedance studies, where a low level of accumulated space charges at temperatures below 150 °C was shown.¹⁶

Polarization retention is an important parameter for characterizing the reliability of ferroelectric thin films for non-volatile memory applications. Retention loss is the reduction in switching or nonswitching polarizations, which can be related to the instability of the two stored logic states (0 and 1). Figure 5(a) shows the hysteresis loops for the BNdT film before and after a retention test for 3.6×10^4 s at 100 °C, demonstrating a little polarization decay. Figure 5(b) plots the evolution of switchable polarization as a function of test duration at both 100 and 150 °C. An apparent initial retention loss was observed at both temperatures, likely due to the fast depolarization effect.²⁵ The polarization then becomes more or less stabilized with an elongated relaxation time. At

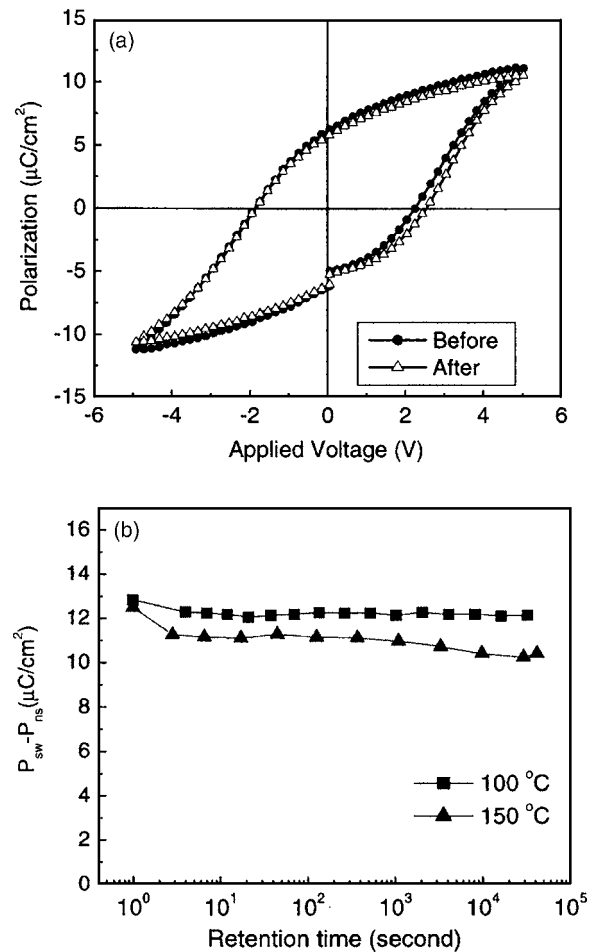


FIG. 5. (a) Hysteresis loops before and after 3.6×10^{10} s of retention test at 100 °C, and (b) retained polarization ($\Delta P = P_{\text{sw}} - P_{\text{ns}}$) as a function of retention time tested at both 100 and 150 °C for the BNdT film.

100 °C, the polarization shows little degradation up to 3.6×10^4 s. When the temperature is raised to 150 °C, the retention loss is accelerated, as demonstrated by a retention loss of ~8% upon 10 h of retention test. Retention loss is generally related to the residual depolarization field and other built-in voltages arising from space charges, resulting in reversal of some unstable domains.^{25–29} At higher temperatures, domain reversals are accelerated due to the thermal activation, leading to polarization degradation. In comparison to PZT and SBT capacitors with Pt electrodes, the retention loss observed for BNdT films in this work is relatively smaller.^{26,27} The improved retention resistance suggests that the domains in BNdT are rather stable, which can be accounted for by the relatively large coercive field observed for BNdT, in combination with a low level of space charges, as mentioned above.

To study the imprint behaviors of the BNdT thin films deposited by sputtering in this work, they were first poled at 5 V at room temperature, and then baked at 100 °C for 3.6×10^4 s. Figure 6(a) plots the hysteresis loops for the BNdT films that were positively and negatively poled, together with that for the unpoled one as a reference. There is an apparent left shift in the hysteresis loop for the positively poled film, while there is a right shift for the negatively poled thin film upon 10 h of imprint test. These shifts in hysteresis loop can

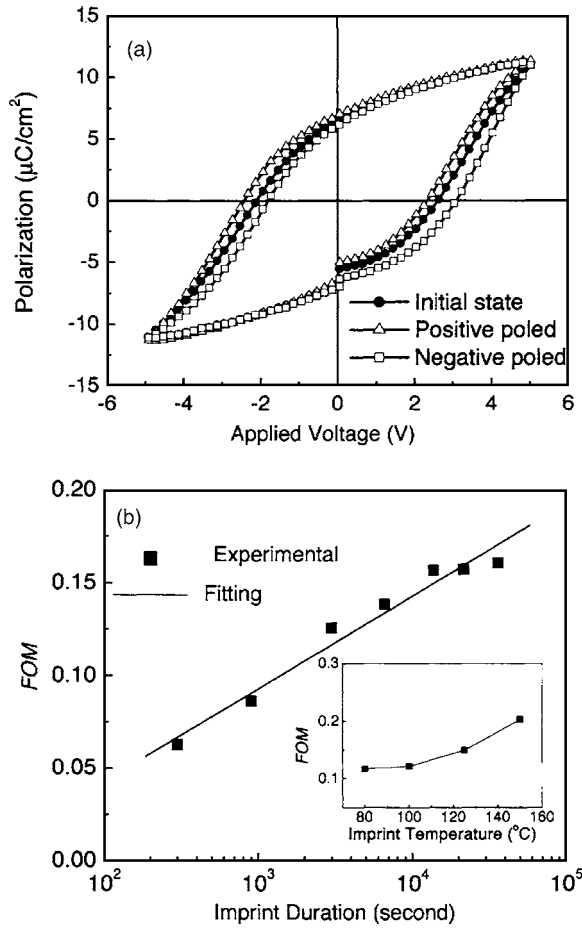


FIG. 6. (a) Hysteresis loops for the BNdT film after negative- and positive-poled imprint tests at 100 °C for a duration of 3.6×10^4 s, together with the unpoled one as a reference, and (b) figure of merit (FOM: $\text{FOM} = [(+V_c^{\text{final}}) + (-V_c^{\text{final}})] / [(+V_c^{\text{int}}) - (-V_c^{\text{int}})]$) against imprint duration for the BNdT film. The insert shows the evolution of FOM after imprint at different temperatures for 2 h.

be accounted for by the occurrence of an internal bias field. To present a semiquantitative analysis of such behavior, figure of merit (FOM) can be used to quantify the degree of asymmetry of hysteresis loops, which is given by the equation

$$\text{FOM} = \frac{(+V_c^{\text{final}}) + (-V_c^{\text{final}})}{(+V_c^{\text{int}}) - (-V_c^{\text{int}})},$$

where (V_c^{int}) and (V_c^{final}) are the coercive voltages before and after baking, respectively, and $\text{FOM} = \pm 1$ denote the imprint failure conditions. As shown in Fig. 6(b), FOM shows a more or less logarithmical increase against the test time. Upon completion of the imprint test at 3.6×10^4 s, FOM has grown up from around 0.06 at the initial state to a final state of ~ 0.16 , indicating a desirable imprint resistant behavior. To further study the temperature effect, FOM was measured at various imprint temperatures for 2 h. As expected, the amount of imprint increases with rising temperature (shown in the insert), demonstrating an obvious imprint acceleration behavior by heating. While the imprint phenomena can be related to several different mechanisms, e.g., alignment of the defect dipoles, internal bias from bulk space-charge screening mechanisms, and interfacial layer space-charge

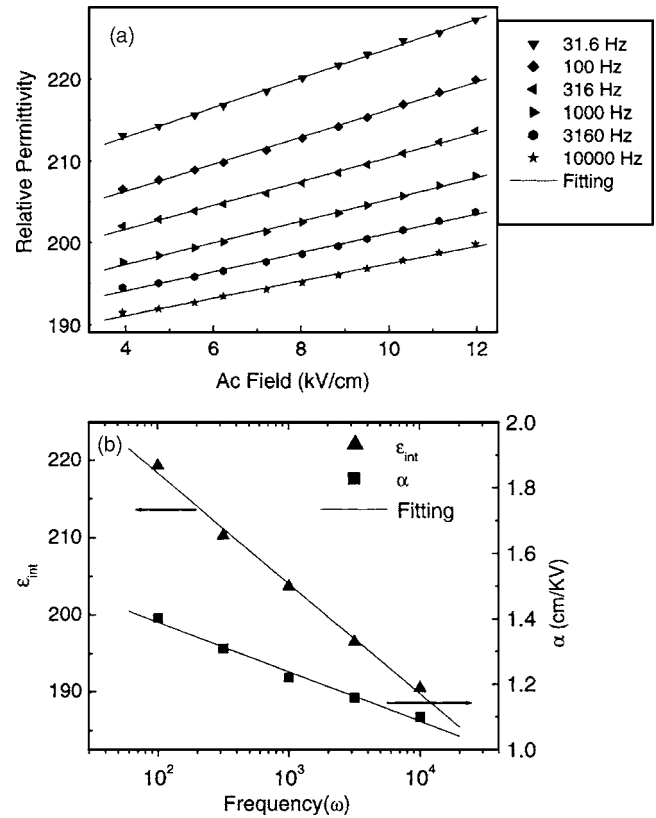


FIG. 7. (a) ac dependence of relative permittivities, together with fitting results by Rayleigh equation at various frequencies, and (b) reversible and irreversible Rayleigh parameters as a function of frequency for the BNdT film.

screening,^{29–34} the relative smaller imprint observed for the BNdT thin film in this work is attributed to the limited defect-induced space charges, together with the high coercive field shown.

Figure 7(a) shows the relative permittivity of the BNdT thin film, deposited by sputtering and then annealed at 700 °C, as a function of ac-driven voltage. At each frequency studied in the range of around 100–10 000 Hz, the relative permittivity demonstrates a linear relationship with the applied ac field, which can be fitted into the Rayleigh relation $\varepsilon_0 = \varepsilon_{\text{int}} + \alpha E$, where ε_{int} corresponds to the contributions from intrinsic lattice and reversible domain wall, while αE corresponds to the contributions from irreversible domain-wall movements.^{23–25} By fitting the dielectric behaviors into the Rayleigh equation, ε_{int} and α can be extracted and plotted as a function of frequency, as shown in Fig. 7(b). Both ε_{int} and α decrease linearly with the logarithm of frequency, which can be expressed as $\varepsilon_{\text{int}} = \varepsilon_0 - \beta_1 \ln(\omega)$ and $\alpha = \alpha_0 - \beta_2 \ln(\omega)$, where $\varepsilon_0, \alpha_0, \beta_1$, and β_2 are constants, and ω is test frequency. As a result of the logarithmic decrease in both reversible and irreversible components, the relative permittivity thus shows a similar logarithmic frequency-dependent behavior. This further confirms that the dielectric nonlinearities of the BNdT film are related to the domain-wall pinning effect, which has been reported for PZT and other oxide ceramic thin films,^{35–39} where an apparent change in both reversible and irreversible components was observed in PZT after fatigues.⁴⁰ The domain pinning arises from structural

defects such as oxygen vacancies or interfacial defects, which act as obstacles impeding domain-wall movement, leading to a reduction in the irreversible component of relative permittivity.

IV. CONCLUSIONS

rf sputtering and subsequent thermal annealing at 700 °C have been successfully employed to deposit $(\text{Bi}_{3.15}\text{Nd}_{0.85})\text{Ti}_3\text{O}_{12}$ (BNdT) thin films of random orientation on a Pt/Ti/SiO₂/Si substrate. The resulting BNdT thin film demonstrates a well-established ferroelectric hysteresis loop, where a remanent polarization $2P_r$ of 23.2 $\mu\text{C}/\text{cm}^2$ and a coercive field E_C of 112 kV/cm were measured at 10 V. It exhibits a nonswitchable polarization of 12.9 $\mu\text{C}/\text{cm}^2$ at room temperature, together with an almost fatigue-free behavior up to more than 10^{10} switching cycles at both 100 and 150 °C. Desirable retention and imprint behaviors were observed at 100 °C, although the retention loss and imprint were accelerated by an increase in temperature to 150 °C. The relative permittivity shows a linear correlation with respect to ac electrical field, which can be fitted by the Rayleigh law, indicating the domain-wall pinning by defects in the BNdT thin films.

ACKNOWLEDGMENTS

This paper is based upon work supported by the Science and Engineering Research Council - A*Star, Singapore, under Grant No. 022 107 0007. The authors also acknowledge the support of the National University of Singapore.

- ¹R. Ramesh, S. Aggarwal, and O. Auciello, *Mater. Sci. Eng.*, **R. 32**, 191 (2001).
- ²T. Mikolajick, C. Dehm, W. Hartner, I. Kasko, M. J. Kastner, N. Nagel, M. Moert, and C. Mazure, *Microelectron. Reliab.* **41**, 947 (2001).
- ³C. A. Paz de Araujo, J. D. Cuchiaro, L. D. McMillan, M. C. Scott, and J. F. Scott, *Nature (London)* **374**, 627 (1995).
- ⁴L. Geppert, *IEEE Spectrum* **40**, 48 (2003).
- ⁵J. F. Scott, *Ferroelectric Memories* (Springer, New York, 2000).
- ⁶A. Kingon, *Nature (London)* **401**, 658 (1999).
- ⁷B. H. Park, B. S. Kang, S. D. Bu, T. W. Noh, J. Lee, and W. Jo, *Nature (London)* **401**, 682 (2002).
- ⁸R. Ramesh and D. G. Schlom, *Science* **296**, 1975 (2002).
- ⁹U. Chon, H. M. Jang, M. K. Kim, and C. H. Chang, *Phys. Rev. Lett.* **89**, 087601 (2002).
- ¹⁰H. Uchida, H. Yoshikawa, I. Okada, H. Matsuda, T. Lijima, T. Watanabe, T. Kojima, and H. Funakubo, *Appl. Phys. Lett.* **81**, 2229 (2002).
- ¹¹D. Wu, Y. D. Xia, A. D. Li, Z. G. Liu, and N. B. Ming, *J. Appl. Phys.* **94**, 7376 (2003).
- ¹²H. Uchida, H. Yoshikawa, I. Okada, H. Matsuda, I. Takashi, T. Watanabe, and H. Funakubo, *Jpn. J. Appl. Phys., Part 1* **41**, 6820 (2002).
- ¹³S. T. Zhang, X. J. Zhang, H. W. Cheng, Y. F. Chen, Z. G. Liu, N. B. Ming, X. B. Hu, and J. Y. Wang, *Appl. Phys. Lett.* **83**, 4378 (2003).
- ¹⁴A. Garg, Z. H. Barber, M. Dawber, J. F. Scott, A. Snedden, and P. Lightfoot, *Appl. Phys. Lett.* **83**, 2415 (2003).
- ¹⁵T. Kojima, T. Sakai, T. Watanabe, H. Funakubo, K. Saito, and M. Osada, *Appl. Phys. Lett.* **81**, 2746 (2002).
- ¹⁶X. S. Gao, J. M. Xue, and J. Wang, *J. Appl. Phys.* **97**, 034101 (2005).
- ¹⁷X. S. Gao, Z. H. Zhou, J. M. Xue, and J. Wang, *J. Am. Ceram. Soc.* **88**, 1037 (2005).
- ¹⁸W. J. Takei, N. P. Formigoni, and M. H. Francombe, *Appl. Phys. Lett.* **15**, 256 (1969).
- ¹⁹M. Kanaka, T. Higuchi, K. Kudou, and T. Tsukamoto, *Jpn. J. Appl. Phys., Part 1* **41**, 1536 (2002).
- ²⁰N. Ichinose and M. Nomura, *Jpn. J. Appl. Phys., Part 1* **35**, 4960 (1996).
- ²¹H. N. Al-Shareef, D. Dimos, T. J. Boyle, W. L. Warren, and B. A. Tuttle, *Appl. Phys. Lett.* **68**, 690 (1996).
- ²²A. Q. Jiang, J. F. Scott, M. Dawber, and C. Wang, *J. Appl. Phys.* **92**, 6756 (2002).
- ²³M. Dawber and J. F. Scott, *Appl. Phys. Lett.* **76**, 1060 (2000).
- ²⁴H. M. Duiker, P. D. Beale, J. F. Scott, C. A. Paz De Araujo, B. M. Meinick, J. D. Cuchiaro, and L. D. McMillan, *J. Appl. Phys.* **68**, 5783 (1990).
- ²⁵J. M. Benedetto, R. A. Moore, and F. B. McLean, *J. Appl. Phys.* **75**, 460 (1994).
- ²⁶M. Gruverman and M. Tamaka, *J. Appl. Phys.* **89**, 1836 (2001).
- ²⁷B. S. Kang, J.-G. Yoon, T. W. Noh, T. K. Song, S. Seo, Y. K. Lee, and J. K. Lee, *Appl. Phys. Lett.* **82**, 2124 (2004).
- ²⁸A. Z. Simões, M. A. Ramirez, N. A. Perruci, C. S. Riccardi, E. Longo, and J. A. Varela, *Appl. Phys. Lett.* **86**, 112909 (2005).
- ²⁹A. K. Tagantsev, I. Stolichnov, N. Setter, and J. S. Cross, *J. Appl. Phys.* **96**, 6616 (2004).
- ³⁰M. Grossmann, O. Lohse, D. Bolten, U. Boettger, and T. Schneller, *J. Appl. Phys.* **92**, 2680 (2002).
- ³¹K. Ashikaga, K. Takaya, T. Kanehara, and I. Ko, *Appl. Phys. Lett.* **86**, 162901 (2005).
- ³²W. L. Warren, D. Dimos, G. E. Pike, B. A. Tuttle, R. Ramesh, and J. T. Evans, Jr., *Appl. Phys. Lett.* **67**, 866 (1995).
- ³³S. Sadashivan, S. Aggarwal, T. K. Song, R. Ramesh, J. T. Evans, Jr., B. A. Tuttle, W. L. Warren and D. Dimos, *J. Appl. Phys.* **83**, 2165 (1998).
- ³⁴S. Aggarwal, I. G. Jenkins, B. Nagaraj, C. Canedy, R. Ramesh, G. Velasquez, L. Boyer, and J. T. Evans, Jr., *Appl. Phys. Lett.* **75**, 1787 (1999).
- ³⁵D. Bolten, U. Böttger, T. Schneller, M. Grossmann, O. Lohse, and R. Waser, *Appl. Phys. Lett.* **77**, 3830 (2000).
- ³⁶D. Bolten, U. Böttger, and R. Waser, *J. Appl. Phys.* **93**, 1735 (2003).
- ³⁷D. Damjanovic, *Phys. Rev. B* **55**, R649 (1997).
- ³⁸C. R. Cho, W.-J. Lee, B.-G. Yu, and B.-W. Kim, *J. Appl. Phys.* **86**, 2700 (1999).
- ³⁹O. Boser, *J. Appl. Phys.* **62**, 1344 (1987).
- ⁴⁰J. L. Sun, J. Chen, X. J. Meng, J. Yu, L. X. Bo, S. L. Guo, and J. H. Chu, *Appl. Phys. Lett.* **80**, 3584 (2002).